JOURNAL OF THERMOPHYSICS AND HEAT TRANSFER
Vol. 18, No. 2, April–June 2004

Radiative Characteristics of Opaque Spherical Particles Beds: A New Method of Prediction

R. Coquard*
Centre Scientifique et Technique du Bâtiment, 38400 Saint Martin d'Hères, France
and
D. Baillis†
Centre de Thermique de Lyon, 69621 Villeurbanne CEDEX, France

The aim of this paper is to present a new method to compute the radiative characteristics of spherical particles beds. This method is applied to beds made of opaque diffusely or specularly reflecting particles with size parameters ranging in the geometric optics limit. It is based on a Monte Carlo procedure, and no hypotheses are made on dependent or independent scattering regime. Thus, the limits of validity of independent scattering hypothesis are investigated. Firstly, we present the principle and the hypothesis of the method. It is then applied to different beds and permits us to analyze the evolution of the extinction coefficient, scattering albedo, and phase function of the bed with the porosity and with the reflecting properties of the particles. Thereafter, the radiative characteristics obtained are compared to those predicted by the correlations issued from the literature. Our results proves to be very close to those of predicted by the correlation of Kaviany and Singh but somewhat different from the results of Kamiuto's correlation. Finally, the hemispherical transmittances of packed beds are calculated using the discrete ordinate method and compared to the experimental results of Chen and Churchill and to theoretical results issued from literature.

Nomenclature

c	=	average interparticle clearance
d	=	distance between the center of two neighboring particles
$\mathrm{d}\omega(\theta_i')$	=	solid angle around direction θ_i'
G	=	random generated number
$I(y, \mu)$	=	luminance at the abscissa $y(m)$ in the direction μ
N_{part}	=	number of particles per unit volume of the bed
n	=	refractive index of the particle
$P(\beta)$	=	scattering phase function
R	=	radius
S_{part}	=	cross section of the particles
T	=	hemispherical transmittance
x	=	size parameter of the particle ($x = 2\pi R_{\text{part}}/\lambda$)
y_0	=	thickness of the packed bed
α	=	angle between intercepted ray and the normal to the surface of the particle, rad
β	=	extinction coefficient, m^{-1}
ε	=	porosity
θ	=	angle between the starting ray and the ray scattered away from the sphere, rad
θ'	=	angle between intercepted and reflected rays at the surface of the particle, rad
λ	=	wavelength, m
μ	=	directing cosine
$\rho_\lambda(\alpha, n)$	=	reflectivity of the specularly reflecting particles
$\bar{\rho}$	=	hemispherical reflectivity
ω	=	scattering albedo

Subscripts

bed	=	of the bed
ho	=	isotropic and homogeneous absorbing and scattering medium
ind	=	from independent scattering theory
part	=	of the particle
sphere	=	of the sphere

Received 9 September 2003; revision received 24 October 2003; accepted for publication 24 October 2003.

*Ph.D. Student, 24 rue Joseph Fourier; r.coquard@cstb.fr.
†Assistant Professor, UMR CNRS 5008, Domaine Scientifique de la Doua, INSA de Lyon, Bâtiment Sadi Carnot, 9 rue de la physique.

I. Introduction

RADIATIVE heat transfer has been proven to play a significant part in the total heat transfer through packed and fluidized beds. In many engineering applications, it is then necessary to understand well and model the radiation–material interaction phenomenon occurring in that kind of medium. Recent works on this subject comprise both independent and dependent scattering studies.[1]

The independent scattering hypothesis is satisfied if the following are there:

1) There is no interference between the scattered waves (far-field effects). This leads to a limit on the minimum value of c/λ.

2) Particles behave as point scatterers (near-field effects are neglected). That is, the distance between neighboring particles is large compared to their sizes. Thus, each particle scatters as if it were alone. This leads to a low limit value of the porosity.

In the case of dependent scattering, interparticle effects should be accounted for in the calculation of the assembly radiative characteristics. These effects involve the following:

1) Far-field effects result from interference between the waves scattered by the particles with phase difference. They only affect the scattering characteristics of the medium.

2) Near-field effects are the effects of multiple scattering in an elementary volume in which the scattering and absorption characteristics of a particle are affected by the proximity of other particles.

The limits of applicability of the theory of independent scattering have been experimentally investigated since the beginning of the 1970s by several authors, including Hottel et al.,[2] Ishimaru and Kuga,[3] and Brewster.[4] Brewster[4] and Yamada et al.[5] proposed a single criterion based on the value of the dimensionless number c/λ.Their results indicated that no dependent effect occurs as long as $c/\lambda > 0.3$ or 0.5.

Singh and Kaviany[6] examined dependent scattering in packed beds of large-size particles (geometric optics domain) by carrying out Monte Carlo simulations. The Monte Carlo simulations for different porosities are compared with available experimental results

and also with the results obtained from the solution of the radiative-transfer equation (RTE) derived under assumption of independent scattering. The independent theory is shown to fail for systems with low porosity even when the c/λ criterion is satisfied. The failure is more drastic for transmission through beds of opaque spheres than for transparent and semitransparent spheres. For the same particle radiative characteristics, the deviation from the independent theory is shown to increase with a decrease in the porosity. The deviation from the independent theory can be significant even for porosities as high as 0.935.

Different methods have been proposed in order to take into account the dependent scattering of spherical particles:

1) Kamiuto[7] and Kamiuto et al.[8] have proposed an heuristic correlated-scattering theory for packed beds consisting of relatively large spheres. The extinction coefficient and the albedo are scaled by a factor γ such that

$$\beta = \gamma \times \beta_{\text{independent}} \qquad \text{and} \qquad \omega = 1 - (1 - \omega_{\text{independent}})/\gamma$$

where

$$\gamma = 1 + \tfrac{3}{2} \times (1 - \varepsilon) - \tfrac{3}{4} \times (1 - \varepsilon)^2 \qquad \text{for} \qquad \varepsilon < 0.921$$

The absorption-efficiency factor is assumed to be identical with the uncorrelated absorption-efficiency factor. The phase function is left unchanged from the independent scattering case. For opaque particles, the uncorrelated radiative characteristics are determined by a combination of the geometric optics laws and of diffraction theory from hemispherical reflectivity of particles.[7] Using this correlation, the authors calculated the hemispherical transmittances of randomly packed beds of spheres under the conditions corresponding to the experiments of Chen and Churchill. They found that their correlation provides much better agreement with the Chen–Churchill experiments than the results obtained from independent scattering theory.

In Ref. 8, the authors applied the geometric optics theory to alumina or stainless-steel spheres. The albedos and the asymmetry factors

$$\left(\tilde{g} = 0.5 \times \int_{-1}^{1} P(1, \mu')\mu' \, \mathrm{d}\mu'\right)$$

of the phase functions of packed beds of stainless steel and alumina have been also determined experimentally by using the emerging intensity fitting method. The experimental results are compared with theoretical predictions based on these authors correlated scattering theory. It has been found that the albedos obtained are close to the theoretical predictions, but the measured values of the asymmetry factors significantly differ from the predicted values derived from this theory.

2) Kaviany and Singh[9] and Singh and Kaviany[10] have presented a method for modeling dependent radiative heat transfer through beds of large spherical particles. Such a system of large spheres lies in the dependent range (multiple scattering) even for large porosities. The dependent characteristics for a bed of opaque spheres are obtained from their independent characteristics by scaling the optical thickness while leaving the albedo and the phase function unchanged. The scaling factor S_r is calculated by finding the ratio of the slopes calculated by the Monte Carlo method and by independent theory. S_r is found to depend only on the porosity and is almost independent on the emissivity. The values of S_r are fitted as follows:

$$S_r = 1 + 1.84 \times (1 - \varepsilon) - 3.15 \times (1 - \varepsilon)^2 + 7.2 \times (1 - \varepsilon)^3 \qquad \text{for} \qquad \varepsilon > 0.3$$

It is shown that such a simple scaling for nonopaque particles is not feasible.

These authors have also compared their results with those of Kamiuto[7] obtained from the correlated scattering theory (just reported). In this case, the results do not generally show good agreement with the results obtained with the Monte Carlo method.

3) In Jones et al.,[11] the radiation intensity exiting a heated, nonisothermal packed bed of monodispersed, opaque, large spherical particles (1 mm diameter, porosity of 0.37) with boundary emission and reflection is measured spectrally and directionally using a radiometric technique. The authors compared measured and computed intensities. The bed is considered one dimensional and optically thick, and is submitted to known constant temperature boundary conditions. Intensity exiting the bed is numerically simulated by using a discrete ordinates solution to the RTE, coupled to a solution of the energy conservation. Radiative characteristics are obtained by using the geometric optics and diffraction correlated scattering theory derived by Kamiuto[7] and Kamiuto et al.[8] It is found that measured and computed intensities agree quite well in near-normal directions. However, the values of measured and computed intensities diverge as the polar angle is increased beyond about 48 deg, with the measured results showing a strong directional character, while the computed results are almost diffuse. Intensities computed with radiative characteristics obtained from independent scattering theory demonstrated that independent scattering does not hold in this case. This suggests that either radiative transfer near the boundaries of this medium might not be adequately represented by a continuous form of the RTE or that the characteristics derived from correlated scattering theory are not adequate.

4) In a recent work, Baillis and Sacadura[12] compared measured directional spectral emissivity to theoretical predictions for an isothermal medium made of a dispersion of large oxidized bronze (opaque) spherical particles. Two porosities are tested 0.31 with sphere diameter 300 μ and 0.39 with sphere diameter 400 μm. Comparison between experimental and theoretical emittance results tend to show that Singh and Kaviany's correlation is suitable and necessary.

As can be seen, most of these works have investigated the limit of the independent theory and obtained correlations designed to determine the radiative characteristics of the beds. They were particularly interested in the evolution of extinction efficiency, but the different correlations proposed lead to noticeably different results. Moreover, as regards the evolution scattering parameters (albedo and phase function), especially the albedo, their conclusions are somewhat different, and several hypothesis are made.

We then have developed a new method to identify the extinction efficiency as well as the scattering albedo and phase function of beds of large, opaque, spherical particles. The method is based on a Monte Carlo procedure applied to beds of randomly positioned particles. The porosity of the beds ranges from 1 to 0.53.

First, the hypothesis and the principle of the method are explained in detail, and the accuracy of the method is discussed. Thereafter, we present the results of the identification for beds of opaque spheres with varying reflectivities. The limit of application of independent scattering hypothesis is investigated. Moreover, the radiative characteristics obtained are compared to those predicted by the correlations of Kamiuto et al. and Kaviany and Singh.

Finally, the hemispherical transmittances of packed beds of alumina are calculated from the radiative characteristics obtained by our method and using the DOM. The results are compared to the experimental results of Chen and Churchill.[13]

II. Description of the Method

A. Hypotheses

Several hypotheses are employed in order for our method to be applicable. First, we suppose that the radius R_{part} of the spherical particles of the beds is much greater than the wavelength λ of the thermal radiation studied. For a radiative heat-transfer calculation at 300 K, the wavelength concerned range between 5 and 25 μm. We will consider beds made of particles with radius greater than 100 μm.

The size parameter x of such particles is much greater than one, and then the radiation–matter interaction could be treated using the geometric optics laws.

Moreover, the influence of diffraction on the radiative heat transfer is neglected. Indeed, the diffraction phase function for large particles is predominantly oriented in the forward direction, and diffracted rays are very close to transmitted rays. We then assume, here, that diffraction can be treated as transmission.

Given that the medium is made of randomly positioned spherical particles, we also assume that all of the properties are independent on the azimuth angle (azimuthal symmetry).

Finally, we suppose that the particles contained in the beds are opaque. Our study can take into account two types of particles:

1) The first type of particle consists of large diffusely reflecting spheres: the reflectivity of the particle is the same whatever the direction of incident ray is. This reflectivity is equal to the hemispherical reflectivity $\bar{\rho}$ of the solid phase contained in the particle. Moreover, the rays intercepted by a surface element of a particle could be reflected in all directions of the hemisphere with the same probability.

2) The second type of particle consists of large dielectric (imaginary index $k \ll n$) and specularly reflecting spheres: the specular reflectivity strongly depends on the refractive index n of the solid phase as well as on the angle α between the intercepted ray and the normal to the surface. It could be surprising that the particles are dielectric and opaque too. In fact, the imaginary index k is much smaller than n but not null, and the particles are assumed sufficiently large to consider that the rays entering the particles are all absorbed before leaving it. The reflectivity is then determined using the laws of reflection and refraction for dielectrics given in Ref. 14. We have

$$\rho_\lambda(\alpha, n) = \frac{1}{2}\frac{\sin^2(\alpha-\chi)}{\sin^2(\alpha+\chi)}\left[1+\frac{\cos^2(\alpha+\chi)}{\cos^2(\alpha-\chi)}\right] \tag{1}$$

$$\chi = \sin^{-1}\left[\frac{\sin(\alpha)}{n}\right] \tag{2}$$

Moreover, the angle between the normal to the surface and the reflected ray is equal to the angle between the incident ray and the normal to the surface.

B. Principle of the Method

The principle of the method is to determine the values of the extinction coefficient β_{bed}, the scattering albedo ω_{bed}, and the scattering phase function $P_{\text{bed}}(\theta')$ of the homogeneous isotropic absorbing and scattering medium that best match the radiative behaviour of the beds.

First, we generate beds of spherical particles of infinite length, height, and width and with varying porosity. The beds are made of randomly positioned particles. The porosity of the beds generated varies between 1, when neighboring particles are very distant from each other, and 0.53, for a bed of touching particles.

Then, a Monte Carlo procedure starts and the path of a ray, starting in random points of the bed and with random starting directions, is tracked until it leaves a sphere of radius R_{sphere} centered on the starting point. The choice of the radius of the sphere is discussed thereafter.

The rays can pass through the sphere without being intercepted or undergo one or several reflections at the surface of the particles and be partially absorbed before leaving the sphere. Each time rays are reflected at the surface of a particle the angles θ' between incident and reflected directions are memorized. Moreover, when rays leave the sphere after one or several reflections the angles θ between the starting and scattered directions are also memorized (Fig. 1).

For a great number of rays, we can compute the following:

1) *Trans* is the proportion of the starting energy leaving the sphere without being intercepted (transmitted rays).

2) *Sca* is the proportion of starting energy leaving the sphere after one or several reflection (scattered rays).

3) $E(\theta)$ is the average angular repartition of the energy scattered outside the sphere of radius R_{sphere}. In practice, the repartition is discretized for $\theta_0 = 0$ deg, $\theta_1 = 1$ deg, ..., $\theta_{180} = 180$ deg. Then, all the rays leaving the sphere with an angle θ comprised between $\theta_i - 0.5$ deg and $\theta_i + 0.5$ deg are regrouped in $E(\theta_i)$.

4) $S(\theta')$ is the average angular repartition of the rays reflected by the particles. This repartition is obtained by memorizing every reflecting angle each time a reflection occurs. As for $E(\theta)$, in practice, the repartition is discretized for $\theta'_0 = 0$ deg, $\theta'_1 = 1$ deg, ..., $\theta'_{180} = 180$ deg.

These four parameters entirely describe the radiative behavior of the bed. The characteristics of the bed are computed from these parameters.

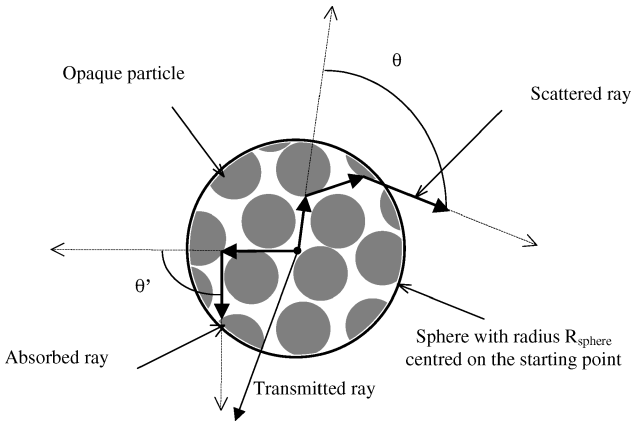

Fig. 1 Monte Carlo procedure in the sphere of radius R_{sphere}.

Indeed, considering the bed as a homogeneous isotropic absorbing and scattering medium, the parameter *Trans* only depends on its homogeneous extinction coefficient β_{bed}. By definition, we have

$$\exp(-\beta_{\text{bed}} \times R_{\text{sphere}}) = Trans$$
$$\Leftrightarrow\ \beta_{\text{bed}} = -\text{Log}(Trans)/R_{\text{sphere}} \tag{3}$$

As regards the scattering phase function of the bed $P_{\text{bed}}(\theta)$, it can be obtained from the discretized angular repartition $S(\theta')$ calculated from the Monte Carlo procedure. Indeed $S(\theta')$ represents, in fact, the probability for an incident ray to be scattered in a direction making an angle comprised between $\theta' - 0.5$ deg and $\theta' + 0.5$ deg with the incident direction. Whereas $P_{\text{bed}}(\theta')\,\text{d}\omega$ represents the probability for the incident ray to be scattered in the solid angle dω centered on the direction making an angle $\boldsymbol{\theta}'$ with the incident direction. The discretized scattering phase function is then obtained by

$$P_{\text{bed}}(\theta'_i) = S(\theta'_i)/\text{d}\omega(\theta'_i) \qquad \text{for} \qquad i = 0, \ldots, 180$$

We have

$$\text{d}\omega(\theta'_i) = 2\pi\sin(\theta'_i)\Delta\theta'_i = 2\pi\sin(\theta'_i) \times 2\pi/360$$
$$\text{for} \qquad i = 0, 180$$

and then

$$P_{\text{bed}}(\theta'_i) = \frac{S(\theta'_i)}{\sin(\theta'_i) \times \pi^2/90} \tag{4}$$

The scattering phase function is then normalized to have

$$\frac{1}{4\pi}\sum_{i=0}^{180} P_{\text{bed}}(\theta'_i) \times 2\pi\sin(\theta'_i)\,\text{d}\theta'_i = 1 \tag{5}$$

Finally, as regards the scattering albedo of the bed, it could not be determined directly. To solve the problem, we apply the same Monte Carlo procedure to an homogeneous, isotropic absorbing and scattering medium having an extinction coefficient $\beta = \beta_{\text{bed}}$ a scattering phase function $P(\theta') = P_{\text{bed}}(\theta')$ and a varying albedo ω. We then compute the parameters $Trans_{\text{ho}}$, Sca_{ho}, and $E_{\text{ho}}(\theta)$, which have the same significance as before, but now concern the isotropic absorbing and scattering medium. An iterative process is then applied in order to determine the value of ω for which $Sca_{\text{ho}} = Sca$. We then have, for the homogeneous absorbing and scattering medium associated with the bed,

$$Trans_{\text{ho}} = Trans, \qquad Sca_{\text{ho}} = Sca \qquad \text{and} \qquad S_{\text{ho}}(\theta') = S(\theta')$$

However, in order for this medium to represent exactly the radiative behavior of the bed the angular repartitions of scattered energy $E(\theta)$ and $E_{\text{ho}}(\theta)$ must be very close to each other. Then, we have also compared the angular repartition of the energy scattered away from the sphere $E(\theta)$ and $E_{\text{ho}}(\theta)$ for the beds studied.

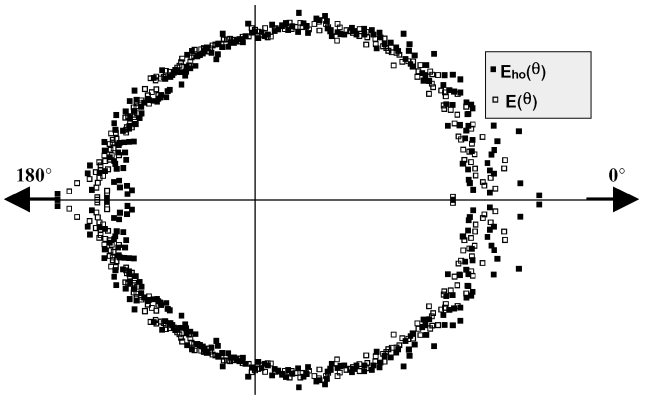

Fig. 2 Comparison of the average angular repartition of the energy scattered away from the spheres for a bed of diffusely reflecting particles with porosity of 0.8517 and for the associated homogeneous absorbing and scattering medium.

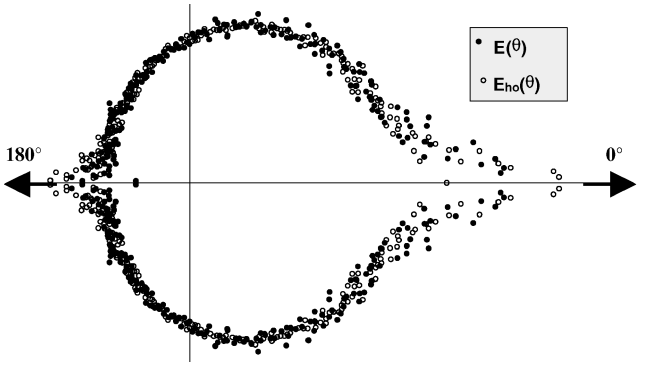

Fig. 3 Comparison of the average angular repartition for a bed of specularly reflecting particles with porosity of 0.7615 and for the associated homogeneous absorbing and scattering medium.

Figures 2 and 3 depict these repartitions for a bed of diffusely reflecting particles with porosity 0.85172 and a bed of specularly reflecting spheres with porosity 0.76156. On both figures, the points in the lower half of the curve are simply repeated points from the upper half.

As can be seen, in both cases $E(\theta)$ and $E_{\text{ho}}(\theta)$ are very close to each other. The fluctuations observed are mainly caused by the Monte Carlo procedure, which generates random numbers to determine the path of the rays. These fluctuations are more pronounced for the directions close to 0 and 180 deg for which the solid angle is small, and then the energy collected during Monte Carlo procedure is small. They could be noticeably reduced by increasing the number of rays that would also increase the computation time. We then can conclude that the behavior of the homogeneous absorbing and scattering medium associated with the bed studied match the radiative behavior of the bed very well.

C. Generation of the Beds

Our program permits the generation of beds of varying porosities. The particles in the beds are randomly positioned. The variable R_{part} and d, which respectively correspond to the radius of the particles and to the distance between the centers of two neighboring particles, are the two parameters that entirely describe the arrangement and from which beds are generated. The beds used for the Monte Carlo procedure must have infinite length, height, and width in order for the Monte Carlo procedure to be applicable from any starting point. However, to limit the memory requirement as well as the computational time we considered that the whole bed is made up by several identical samples, contained in parallelepipedal boxes, which are arranged side by side (see Fig. 4). This sample must contain enough particles to be representative of the morphology of real beds.

Table 1 Porosities of the beds studied with the corresponding value of nonunit number d/R_{part}

d/R_{part}	Porosity ε for random particle
10	0.99602
7	0.98884
4	0.93975
3	0.8572
2.5	0.76153
2.3	0.70197
2.2	0.65777
2.1	0.60596
2	0.53094

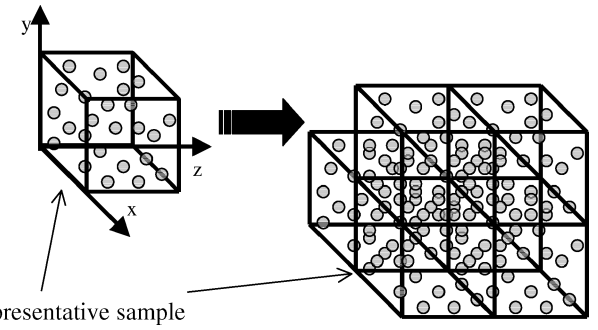

Fig. 4 Generation of the arrangement from one representative sample.

The representative sample is obtained from one ball placed at its center. Several neighboring balls of radius R_{part} are then randomly generated at a distance d from this first one and so on. These particles could be totally or partially contained in the representative sample. Moreover, each time a particle is generated, the program verifies that it is not too close to previously generated particles and to the particles belonging to the neighboring representative samples. For example, for a bed of touching spheres the particles generated should not intersect the other particles. Otherwise, the particle is erased, and another particle is generated.

By this manner beds with infinite length, width, and height are created. Moreover, no discontinuity of the arrangement is found at the boundary of neighboring representative samples.

The porosity of the beds generated is strongly dependent on the dimensionless number d/R_{part}. The larger is d/R_{part}, the larger is the porosity. For a bed of randomly generated touching spheres, a porosity of 0.53 is reached. By comparison, for a regularly packed bed of touching spheres the porosity is equal to $(1-4\pi/3)/8 \approx 0.48$. In Table 1, we have represented the dimensionless number d/R_{part} for the beds studied and their corresponding porosity for random and beds.

D. Development of the Monte Carlo Procedure

In this paragraph, we describe in detail the development of the Monte Carlo procedure, which permits the computation of the parameters *Trans, Sca*, $E(\theta)$, and $S(\theta')$.

1) A point in the first representative box is randomly chosen. His starting coordinates are determined using random numbers that are independently generated. This starting point must belong to a porosity of the bed; otherwise, another starting point is generated until it belongs to a porosity of the bed. Thereafter, the starting directions of the first rays are randomly chosen using other random generated numbers.

2) Then, the path of the ray is tracked. The ray-tracking procedure starts and determines whether the ray hits one of the particles of the current representative sample or if it reaches one of its boundaries.

a) If the ray hits a particle, the procedure determines its new coordinates (the coordinates of the hitting point).

i) If the ray had left the sphere of radius R_{sphere}, then the following can occur:

If the current ray has never been reflected, the parameter *ntrans* is incremented, the procedure goes back to operation 1, and a new ray is generated; or if the current ray has already been reflected one or several times, the angle θ (in degrees) between the starting direction and the leaving direction is calculated, the parameter $Lum(\theta)$ is incremented, the procedure goes back to operation 1, and a new ray is generated.

ii) If the ray is still in the sphere of radius R_{sphere}, the procedure calculates the angle α between the incident ray and the normal to the surface of the particle. The procedure determines the probability for the ray to be reflected. This probability is equal to the reflectivity of the particle. For specularly reflecting particles, the reflectivity $\rho(\alpha, n)$ is determined using the Fresnel relation.[1,2] For diffusely reflecting particles, the reflectivity is equal to the hemispherical reflectivity $\bar{\rho}$ of the particle.

Then, the procedure determines whether the ray is reflected or absorbed using a randomly generated number. If the ray is absorbed, the procedure for the current ray stops, the procedure goes back to operation 1, and a new ray is generated. If the ray is reflected, the procedure determines the reflection angle α'. For specularly reflecting spheres, α' is equal to $-\alpha$, whereas, for diffusely reflecting particles, the reflection angle α' is randomly determined using a random number G by $\alpha' = (G - 0.5) \times \pi$. The parameter $Z(\theta')$ is incremented [where $\theta' = 180 - (\alpha + \alpha')$ is expressed in degrees]. Then the procedure goes back to operation 2 with the new coordinates of the ray and with its new direction.

b) If the ray reaches the boundary of the representative sample, the procedure calculates its new coordinates.

i) If the ray had left the sphere, then the following can occur:

If the current ray has never been reflected, the parameter *ntrans* is incremented, the procedure goes back to operation 1, and a new ray is generated. If the current ray has already been reflected one or several times, the angle θ (in degrees) between the starting direction and the leaving direction is calculated, the parameter $Lum(\theta)$ is incremented, the procedure goes back to operation 1, and a new ray is generated.

ii) If the ray is still in the sphere with radius R_{sphere}, the ray enters the neighboring representative sample with the same direction, and the ray-tracking procedure goes back to operation 2 with the new coordinates of the ray.

The Monte Carlo procedure stops when *compt*, the number of rays generated, is greater than the fixed limit *ntirs*.

The parameter *Trans*, *Sca*, $E(\theta)$, and $S(\theta')$ are calculated by

$$Trans = \frac{ntrans}{ntirs}, \qquad Sca = \frac{\sum_{i=0}^{180} Lum(i)}{ntirs}$$

$$E(\theta) = \frac{Lum(\theta)}{\sum_{i=0}^{180} Lum(i)} \times 4\pi, \qquad S(\theta') = \frac{Z(\theta')}{\sum_{j=0}^{180} Z(j)} \times 4\pi \tag{6}$$

E. Choice of the Radius R_{sphere}

The radius R_{sphere} of the sphere in which the Monte Carlo procedure takes place is an important parameter of the method. We have verified that the values of the radiative characteristics identified are independent on R_{sphere} as long as $R_{\text{sphere}} > d + R_{\text{part}}$. However, the choice of R_{sphere} used for the calculation could have a strong influence on the computation time and the accuracy of the identification. Thus, given that the Monte Carlo procedure uses randomly generated numbers to determine the path of the rays, the angular repartition $S(\theta)$ and $E(\theta)$ calculated during the Monte Carlo procedure undergo fluctuations. The greater is R_{sphere}, the less pronounced these fluctuations are. Indeed, when R_{sphere} is large the number of reflection undergone by the rays before leaving the sphere is more important than for small values of R_{sphere}, and thus the shape of the angular repartition is smoother. Then, the radius R_{sphere} used for the calculation must not be too small.

On the other hand, if R_{sphere} is too large the parameter *Trans* and *Sca* calculated by the Monte Carlo procedure become very small, and the identified values of β_{bed} and ω_{bed} become less precise. Moreover, an increase in the value of R_{sphere} causes an important increase in the computation time.

Table 2 Values of the radius R_{sphere} used for the computation of the radiative characteristics for each bed studied

Porosity ε of the beds	Corresponding value d/R_{part}	R_{sphere} used for the computation
0.99602	10	$70 \times R_{\text{part}}$
0.98884	7	$40 \times R_{\text{part}}$
0.93975	4	$10 \times R_{\text{part}}$
0.8572	3	$8 \times R_{\text{part}}$
0.76153	2.5	$7 \times R_{\text{part}}$
0.70197	2.3	$4 \times R_{\text{part}}$
0.65777	2.2	$3 \times R_{\text{part}}$
0.60596	2.1	$3 \times R_{\text{part}}$
0.53094	2	$3 \times R_{\text{part}}$

For each bed, we then have chosen a value of R_{sphere}, which represents a good compromise between the two antagonists phenomenon. Table 2 shows the values used in this study.

III. Results

A. Evolution of the Extinction Coefficient β_{bed}

The value of the extinction coefficient β_{bed} identified only depends on the porosity ε of the bed and on the radius R_{part} of the particles. It is independent of the reflecting properties of the particles. We also remark that, for a given porosity, the extinction coefficient is proportional to $(R_{\text{part}})^{-1}$. We then have chosen to study the evolution of the dimensionless number $\beta_{\text{bed}} \times R_{\text{part}}$, which only depends on the porosity of the bed.

1. Limit of the Independent Scattering Theory

As regards the dimensionless extinction coefficient, the results of our method are depicted on Fig. 5. The results have been obtained by carrying out several Monte Carlo procedures ($ntirs = 10^6$) for each bed. For each bed, the accuracy of the results has been estimated from the amplitude of the fluctuations of the dimensionless extinction coefficients calculated from the different Monte Carlo procedures. The accuracy of the results is presented using error bars on Fig. 5 and proves to be always lower than 1.5%.

We also have depicted the results of the independent scattering theory. The extinction coefficient β_{ind} is then simply calculated by

$$\beta_{\text{ind}} = N_{\text{part}} \times S_{\text{part}}$$

We have

$$N_{\text{part}} = \varepsilon \Big/ \tfrac{4}{3}\pi R_{\text{part}}^3 \qquad \text{and} \qquad S_{\text{part}} = \pi R_{\text{part}}^2$$

and then

$$\beta_{\text{ind}} \times R_{\text{part}} = \tfrac{3}{4}\varepsilon \tag{7}$$

As can be seen, the dimensionless extinction coefficient calculated by our method rapidly increases when the porosity of the beds decreases. This evolution is nonlinear contrary to the evolution predicted by the independent scattering theory.

As expected, for beds of high porosities the results obtained using our method are close to the results of the independent scattering theory.

However, the relative difference between the two method increases rapidly when the porosity decreases and the independent scattering theory underestimates the dimensionless extinction coefficient.

We notice that the difference exceeds 5% when the porosity is lower than 0.98, which corresponds to $d/R_{\text{part}} \cong 6$. This difference reaches 45% for beds of touching spheres. In this case, the use of independent scattering theory then leads to important errors in radiative transfer calculations.

If the dependent scattering regime is defined by $\beta/\beta_{\text{ind}} > 1.1138$ in accord with a criterion given by Hottel et al.,[2] dependent scattering occurs as soon as the porosity of the bed is lower than approximately 0.94. This limit is then even more severe than that of Singh

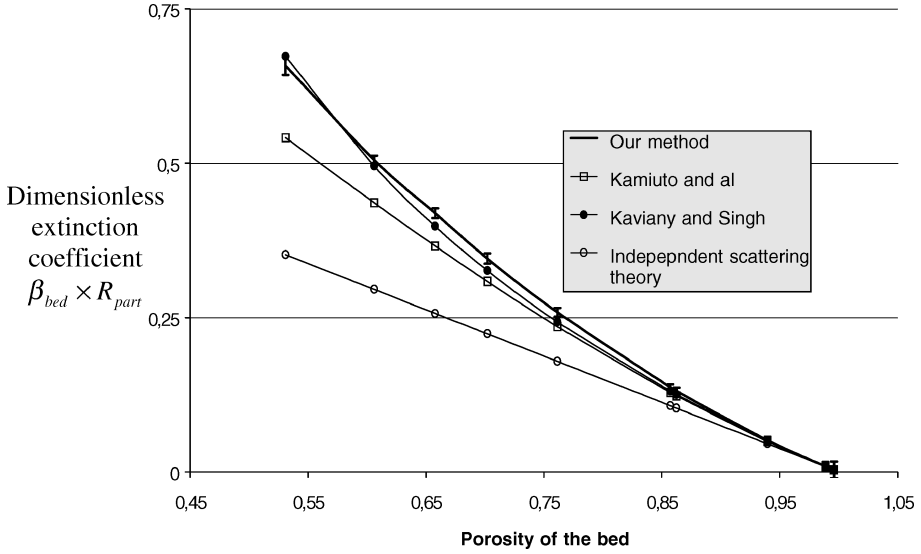

Fig. 5 Comparison of the evolution of the dimensionless extinction coefficient predicted by our method to the evolution predicted by independent scattering theory and by other studies.

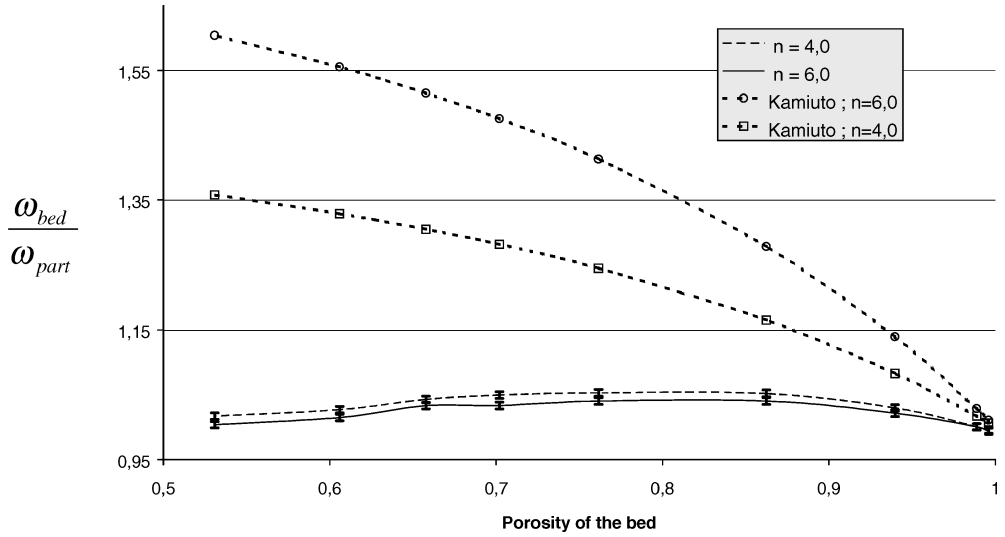

Fig. 6 Comparison of the evolution of the normalized albedo of beds of specularly reflecting spheres obtained from our method to Kamiuto's correlation at $\lambda = 10$ μm.

and Kaviany[6] and Kamiuto et al.,[8] who respectively concluded that independent scattering theory is obsolete when porosity is lower than 0.935 and 0.921.

2. Comparison with Previous Studies

Kaviany and Singh[9] and Kamiuto et al.[8] have proposed scaling correlations in order to determine the extinction coefficient of beds where dependent scattering occurs. These correlations are based on the results of the independent scattering theory and use a scaling factor. They have been presented in the introduction. We have applied these correlations to the beds studied, and the results are compared with the results of our method on Fig. 5.

As can be seen, the dimensionless extinction coefficient predicted by the correlations of Kamiuto and Kaviany and Singh is greater than the one predicted by the independent scattering theory. This observation is in agreement with the results of our method.

Moreover, when the porosity is greater than 0.75 the correlations of Kamiuto and Kaviany and Singh prove to be very close to our results. For example, the maximum relative difference between their results and our results is respectively 8 and 5% in this range of porosity.

However, for beds with porosity lower than 0.75, the agreement between Kamiuto's correlation and our results is no more satisfactory. Indeed, the relative difference increases with decreasing porosity and reaches 17% for a bed of touching spheres ($\varepsilon = 0.53$).

On the other hand, the correlation of Kaviany and Singh is always very close to our method for the whole range of porosity. Indeed, the relative difference is always lower than 5%.

In conclusion, as regards the extinction coefficient of the beds, our results are in very good agreement with the prediction of Kaviany and Singh and slightly different from the correlation of Kamiuto.

B. Evolution of the Scattering Properties $\omega_{bed}/\omega_{ind}$ and $P_{bed}(\theta)$

In this paragraph, we choose to study the evolution of the normalized albedo $\omega_{bed}/\omega_{ind}$ in order to compare the evolution of the albedo for particles with different reflecting properties. For diffusely reflecting particles, the albedo of one particle $\omega_{part} = \omega_{ind}$ is equal to its hemispherical reflectivity $\bar{\rho}$, whereas, for specularly reflecting spheres, it depends on the refractive index and on the wavelength λ studied. It can be calculated by integrating the specular reflectivity over all angles of incidence. For the cases shown in Fig. 6 ($\lambda = 10$ μm, $n = 6.0$ and 4.0), we respectively have $\omega_{part} = \omega_{ind} = 0.4946$ and $\omega_{part} = \omega_{ind} = 0.367$.

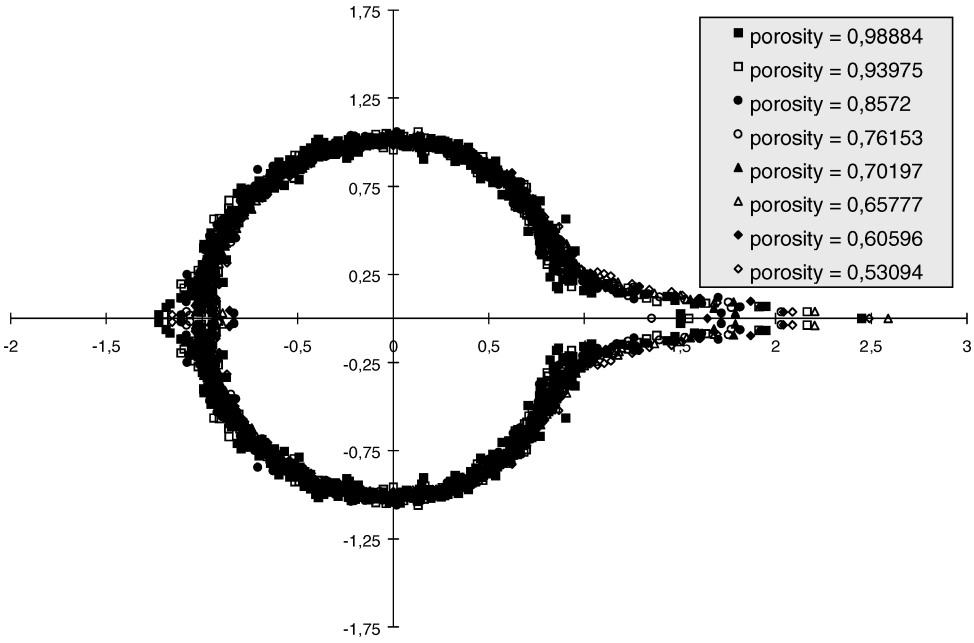

Fig. 7 Evolution of the phase function of beds containing specularly reflecting particles with refractive index $n = 6.0$ at $\lambda = 10$ μm.

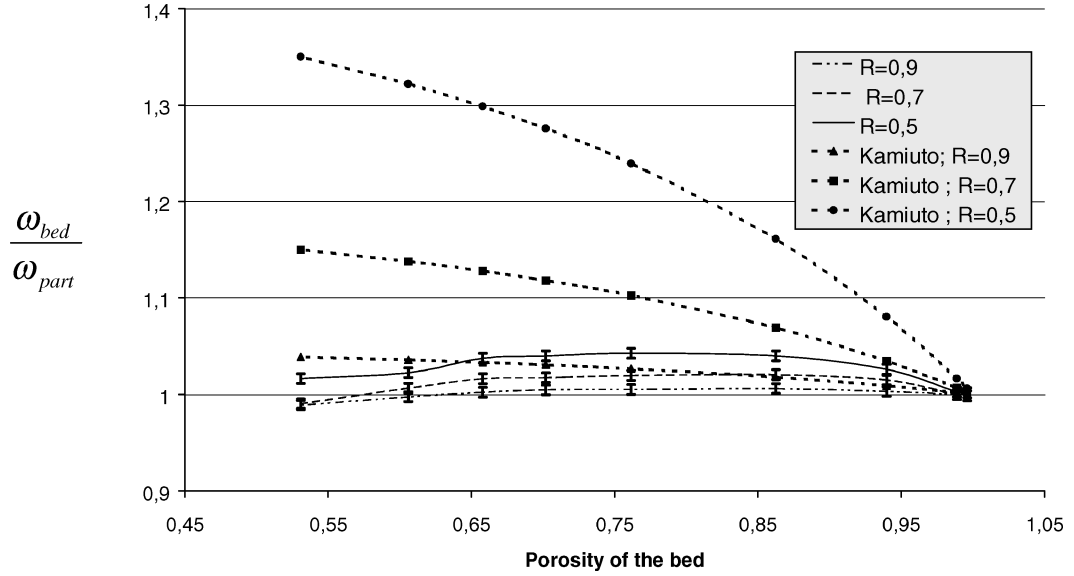

Fig. 8 Comparison of the evolution of the normalized albedo of beds of diffusely reflecting spheres obtained from our method to Kamiuto's correlation.

The evolution of $\omega_{\text{bed}}/\omega_{\text{ind}}$ and $P_{\text{bed}}(\theta)$ with the porosity for beds of specularly and diffusely reflecting particles are depicted in Figs. 6–9. In Figs. 7–9, the points in the lower half of the curve are simply repeated points from the upper half. As for the extinction coefficient, these results have been obtained using several Monte Carlo procedures ($ntirs = 10^6$) for each bed. For the normalized albedo, the accuracy of the results has been estimated from the amplitude of the fluctuations of the albedos identified from the different Monte Carlo procedures. The accuracy of the results are presented using error bars and proves to be always lower than 0.5% for specularly reflecting spheres as well as for diffusely reflecting ones.

As regards scattering phase function of the bed, we notice that it is independent on the porosity. Moreover, this phase function is the phase function predicted by independent scattering theory that is to say the phase function of one particle alone. As was said before, the fluctuations observed are mainly caused by the Monte Carlo procedure, which generates random numbers to determine the path of the rays. These fluctuations are more pronounced for the directions close to 0 and 180 deg for which the solid angle is small, and then the energy collected during Monte Carlo procedure is small. They could be noticeably reduced by increasing the number of rays that would also increase the computation time.

For specularly reflecting particles, the phase function is practically isotropic except for the directions near the forward direction in which rays are predominantly scattered. This phase function is a function of the particle's refractive index n of and of the wavelength of radiation studied. It is expressed in the form[14]

$$P(\theta) = \rho_\lambda[(\pi - \theta)/2, n]/\bar{\rho} \tag{8}$$

On the other hand, for diffusely reflecting spheres the phase function is primarily oriented in the backward direction and is independent on the reflectivity of the particles. Indeed, this phase function is expressed in the form[14]

$$P(\theta) = (8/3\pi)(\sin\theta - \theta\cos\theta) \tag{9}$$

As regards the evolution of the normalized scattering albedo $\omega_{\text{bed}}/\omega_{\text{part}}$ with the porosity, we notice that it mainly depends on

the reflecting properties of the particles. However, the shape of the curves is similar whatever the reflecting properties of the particles are. Thus, when the porosity is close to one the albedo of the bed is close to the albedo of one particle alone given that the independent scattering hypothesis is satisfied. Then, when porosity decreases the albedo of the bed weakly increases and reaches a maximum for a porosity of approximately 0.8. For smaller porosities, the albedo decreases.

The value of the maximum normalized albedo $\omega_{\text{bed}}/\omega_{\text{part}}$ depends on the reflective properties of the particles. Thus, for diffusely reflecting particles as well as for specularly reflecting ones we notice that the less the particles reflect, the higher it is. However, the maximum value of the normalized albedo is always close to one. For example, the maximum value is approximately 1.06 for beds of specularly reflecting spheres with $n = 4.0$ at $\lambda = 10\ \mu$m.

In conclusion, we can say that when dependent scattering occurs the albedo of the bed slightly increases. However, it stays very close to the albedo predicted by independent scattering theory.

The studies of Kamiuto et al. and Kaviany and Singh assumed that the phase function is left unchanged when dependent scattering occurs. Then the results of our method tend to confirm the hypothesis of both authors.

On the other hand, as regards the albedo of the bed, they did not lead to the same conclusions. Indeed, Kaviany and Singh considered that the scattering albedo is left unchanged even when the particles are close to each other, whereas Kamiuto et al. considered that there is an increase of the albedo when dependent scattering occurs. Moreover, they proposed a correlation to calculate the albedo of the bed from the results of independent scattering theory and the porosity of the bed. The correlation has been presented in the introduction. We have compared this correlation with our results in Figs. 6 and 8.

We notice that the albedo predicted by Kamiuto's correlation is always greater than the albedo of independent scattering theory. Moreover, the less the particles reflect, the higher is the albedo. These observations are in good agreement with our results.

However, as can be seen in Figs. 6 and 8, the values of the normalized albedo predicted by Kamiuto is always much greater than the one obtained from our identification method. For example, a normalized albedo of 1.6 is predicted by Kamiuto's correlation for beds of specularly reflecting particles with index $n = 4.0$, whereas the maximum value calculated by our method is 1.06.

Our results are then in better agreement with those of Kaviany and Singh as regards the albedo of the bed.

C. Comparison with Experimental Results of Hemispherical Transmittances

We have also calculated the hemispherical transmittances of a packed bed of alumina spheres under the condition corresponding to the experiment of Chen and Churchill.[13] The physical properties of this packed bed are shown in Table 3. We assumed that the particles in the bed were diffusely reflecting. The boundary conditions corresponding to the experiment are given by

$$I(0, \mu > 0) = 1/\pi, \qquad I(y_0, \mu < 0) = 0 \tag{10}$$

The porosity of the packed bed studied is equal to 0.49, which corresponds to a bed where the particles are slightly compressed. Thus, we have generated a bed of compressed spheres where $d/R_{\text{part}} = 1.932$ (two for noncompressed particles) and $\varepsilon = 0.49$. Thereafter, our method was applied to this bed in order to obtain the radiative characteristics of the homogeneous absorbing and scattering medium associated with the bed.

The one-dimensional radiative transfer equation was then solved using the discrete ordinates method with a quadrature of 180 directions and 50 nodes. The resolution of the luminance field is then very accurate. The hemispherical transmittance was calculated by[14]

$$T = 2\pi \int_0^1 I(y_0, \mu)\mu \, \mathrm{d}\mu \tag{11}$$

The comparison between experimental and theoretical transmittances obtained using our method is shown in Fig. 10. We have also depicted the results of Kamiuto as well as the results of the independent scattering theory and of the correlation of Singh and Kaviany.

We remark that all of the theoretical predictions of the hemispherical transmittances through the packed bed fail to reproduce exactly the behavior of the bed for small values of the dimensionless packed bed thickness. This could be explained by the fact that the theoretical predictions are only applicable to beds with a thickness greater than several diameter of particles.

Table 3 Physical properties of the packed bed of alumina spheres

Parameters	Alumina sphere
Diameter d_p, mm	4.763
Porosity ε	0.49
Number density n_p, sphere/m^3	9.017 E6
Hemispherical reflectivity R	0.72

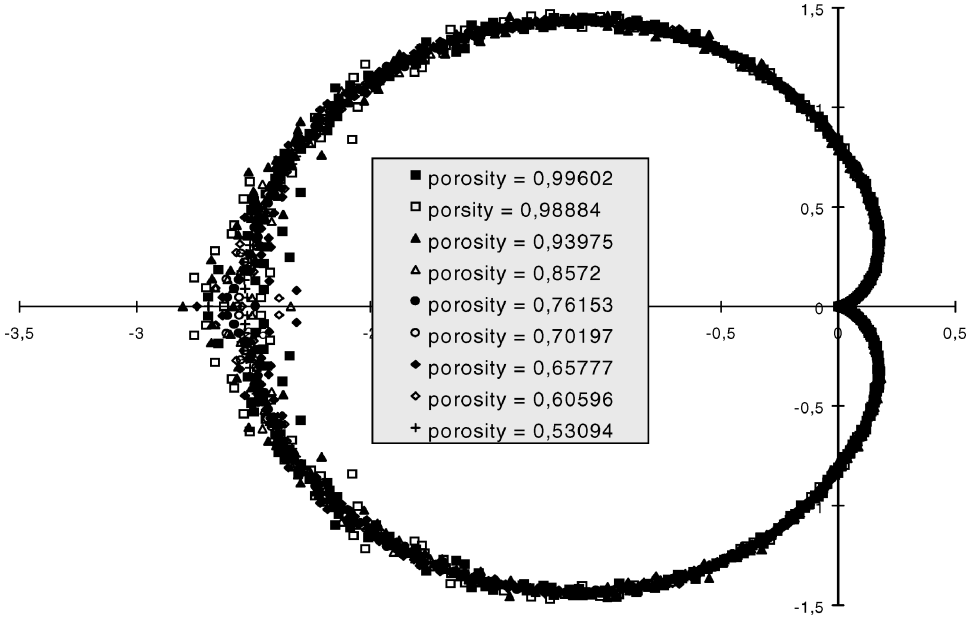

Fig. 9 Evolution of the scattering phase function of beds containing diffusely reflecting particles with the porosity.

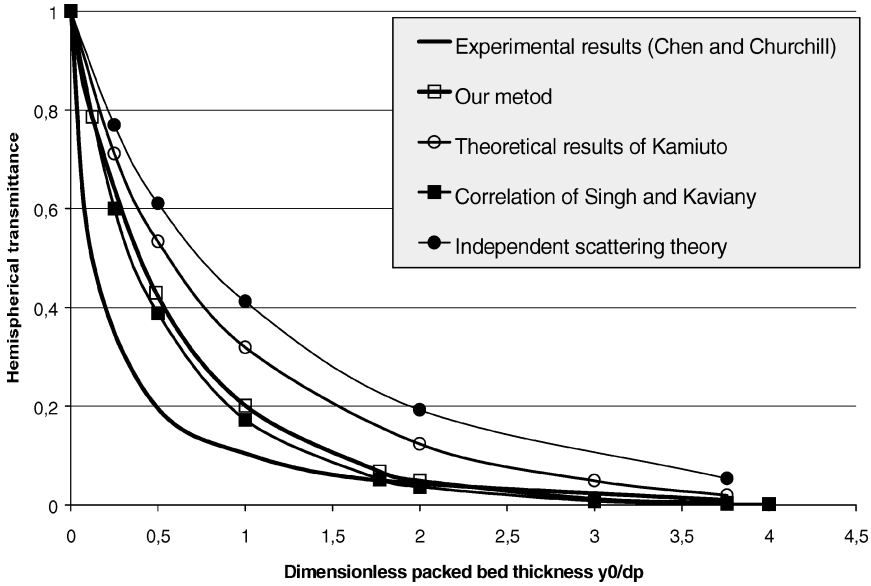

Fig. 10 Comparison of the experimental hemispherical transmittance through a packed bed of alumina spheres, measured by Chen and Churchill, to the theoretical.

However, we notice that the results of the independent scattering theory as well as the results of Kamiuto noticeably overestimate the hemispherical transmittance for the whole range of dimensionless packed bed thickness. On the other hand, the results obtained from our method and from the correlation of Kaviany and Singh, which are very close to each other, are in better agreement with the experimental results. Indeed, as soon as the dimensionless thickness of the bed is greater than 1.5 the values of the hemispherical transmittances predicted by these methods are acceptable when compared to experimental values.

IV. Conclusions

In this paper, we have presented a new method to predict the radiative characteristics of opaque spherical particles beds. It could be used for the whole range of porosity and take into account the dependent scattering effects.

The method has been applied to beds of porosity ranging from 1 to 0.53 containing particles with various reflecting properties. The limit of validity of independent scattering theory has been investigated and proves to be close to that proposed by previous studies.

The radiative characteristics obtained were also compared to those predicted by the correlation of Kamiuto et al. and the correlation of Kaviany and Singh. Both correlations are based on the computation of a scaling factor in order to calculate the real extinction coefficient of the bed from the extinction coefficient of the independent scattering theory. They also assumed that the scattering phase function is left unchanged when dependent scattering occurs. However, as regards the scattering albedo, Kaviany and Singh concluded that it is left unchanged, whereas Kamiuto et al. proposed a correlation to determine the variation of the scattering albedo with the porosity.

The results of the new method prove to be very close to the correlation of Kaviany and Singh. On the other hand, noticeable differences are found with the results of the correlation of Kamiuto et al. as regards the extinction coefficient as well as the scattering albedo.

Thereafter, the hemispherical transmittances through packed beds of opaque diffusely reflecting alumina spheres were calculated using the radiative characteristics obtained by our method and the discrete ordinates method. The results were compared to the experimental results of Chen and Churchill and to theoretical predictions obtained by the other studies in order to estimate the validity of the predictions. It appears that the results of the correlation of Singh and Kaviany and the results of our method are in better agreement with experimental results than the results of the independent scattering theory and the results of the correlation of Kamiuto, which overestimate the transmittance.

Finally, our method could be of great interest given that it could be easily extended to beds of semitransparent particles as well as to heterogeneous media ranging in the geometric optics limit and for which the morphology is known (cellular materials).

References

[1]Baillis, D., and Sacadura, J. F., "Thermal Radiation Properties of Dispersed Media: Theoretical Prediction and Experimental Characterisation," *Journal of Quantitative Spectroscopy and Radiative Transfer*, Vol. 37, 2000, pp. 327–363.

[2]Hottel, H. C., Sarofim, A. F., Dalzell, W. H., and Vasalos, I. A., "Optical Properties of Coatings, Effect of Pigment Concentration," *AIAA Journal*, Vol. 9, 1971, pp. 1895–1898.

[3]Ishimaru, A., and Kuga, Y., "Attenuation Constant of a Coherent Field in a Dense Distribution of Particles," *Journal of the Optical Society of America*, Vol. 72, 1982, pp. 1317–1320.

[4]Brewster, M. Q., "Radiative Heat Transfer in Fluidized Bed Combustors," American Society of Mechanical Engineers, Paper 83-WA/HT-82, 1983.

[5]Yamada, Y., Cartigny, J. D., and Tien, C. L., "Radiative Transfer with Dependent Scattering by Particles: Part 2—Experimental Investigation," *Journal of Heat Transfer*, Vol. 108, 1986, pp. 614–618.

[6]Singh, B. P., and Kaviany, M., "Independent Theory Versus Direct Simulation of Radiation Heat Transfer in Packed Beds," *International Journal of Heat and Mass Transfer*, Vol. 34, No. 11, 1991, pp. 2869–2882.

[7]Kamiuto, K., "Correlated Radiative Transfer in Packed Sphere Systems,"*Journal of Quantitative Spectroscopy and Radiative Transfer*, Vol. 43, No. 1, 1990, pp. 39–43.

[8]Kamiuto, K., Iwamoto, M., Nishimura, T., and Sato, M., "Albedos and Asymmetry Factors of the Phase Function for Packed-Spheres Systems," *Journal of Quantitative Spectroscopy and Radiative Transfer*, Vol. 46, No. 4, 1991, pp. 309–316.

[9]Kaviany, M., and Singh, B. P., "Radiative Heat Transfer in Packed Beds," *Heat and Mass Transfer in Porous Media*, edited by M. Quintard, and M. Todorovic, Elsevier, Amsterdam, 1992, pp. 191–202.

[10]Singh, B. P., and Kaviany, M., "Modelling Radiative Transfer in Packed Beds," *International Journal of Heat and Mass Transfer*, Vol. 35, No. 6, 1992, pp. 1397–1405.

[11]Jones, P. D., McLeod, D. G., and Dorai-Raj, D. E., "Correlation of Measured and Computed Radiation Intensity Exiting a Packed Bed," *Journal of Heat Transfer*, Vol. 118, 1996, pp. 94–102.

[12]Baillis, D., and Sacadura, J. F. "Directional Spectral Emittance of a Packed Bed: Influence of the Temperature Gradient in the Medium," *Journal of Heat Transfer*, Vol. 124, 2002, pp. 904–911.

[13]Chen, J. C., and Churchill, S. W., "Radiant Heat Transfer in Packed Beds," *American Institute of Chemical Engineering Journal*, Vol. 9, 1963, p. 35.

[14]Brewster, Q., *Thermal Radiative Transport and Properties*, 1st ed., Vol. 1, Wiley, New York, 1992.